

1-1-2011

Fully integrated universal biquads using operational transresistance amplifiers with MOS-C realization

AHMET GÖKÇEN

SELÇUK KILINÇ

UĞUR ÇAM

Follow this and additional works at: <https://journals.tubitak.gov.tr/elektrik>



Part of the [Computer Engineering Commons](#), [Computer Sciences Commons](#), and the [Electrical and Computer Engineering Commons](#)

Recommended Citation

GÖKÇEN, AHMET; KILINÇ, SELÇUK; and ÇAM, UĞUR (2011) "Fully integrated universal biquads using operational transresistance amplifiers with MOS-C realization," *Turkish Journal of Electrical Engineering and Computer Sciences*: Vol. 19: No. 3, Article 4. <https://doi.org/10.3906/elk-1002-416>
Available at: <https://journals.tubitak.gov.tr/elektrik/vol19/iss3/4>

This Article is brought to you for free and open access by TÜBİTAK Academic Journals. It has been accepted for inclusion in Turkish Journal of Electrical Engineering and Computer Sciences by an authorized editor of TÜBİTAK Academic Journals. For more information, please contact academic.publications@tubitak.gov.tr.

Fully integrated universal biquads using operational transresistance amplifiers with MOS-C realization

Ahmet GÖKÇEN*, Selçuk KILINÇ, Uğur ÇAM

Department of Electrical and Electronics Engineering, Dokuz Eylül University, Tinaztepe Campus,
Buca, 35160 İzmir-TURKEY

e-mails: ahmet.gokcen@deu.edu.tr, selcuk.kilinc@deu.edu.tr, ugur.cam@deu.edu.tr

Received: 22.02.2010

Abstract

Universal biquadratic filters employing operational transresistance amplifiers are presented. All 5 different second-order filtering functions, namely low-pass, high-pass, band-pass, notch, and all-pass, can be realized. The quality factor of the filters can be adjusted electronically without affecting resonant frequency. The configuration can be made fully integrated based on MOS-C realization, by making use of the current differencing and internally grounded inputs of OTRA. PSpice simulation results are given to verify the theoretical analysis.

Key Words: Analog signal processing, operational transresistance amplifier, MOS-C realization

1. Introduction

Operational transresistance amplifiers (OTRA) are important active elements in analog integrated circuits and systems. Both input and output terminals of OTRA are characterized by low impedance, thereby eliminating the response limitations incurred by capacitive time constants. The input terminals are internally grounded, leading to circuits that are insensitive to the stray capacitances. Thus, it is possible to obtain very accurate transfer functions by using OTRA in contrast to its unity gain active device counterparts. Furthermore, it has been shown that the differential current input nature of this device considerably simplifies the implementation of MOS-C analog integrated circuits [1].

OTRAs are commercially available from several manufacturers under the name of current differencing amplifiers or Norton amplifiers. Recently, they have started to gain considerable attention with the introduction of several high performance CMOS OTRA realizations [1-5], which are simpler and more efficient than the commercially available ones. Many applications of OTRA have been reported in the literature [1-15]. They include universal filters, single-resistance-controlled oscillators, immittance simulators, and all-pass filters. On the other hand, a literature survey shows that both Kerwin-Huelsman-Newcomb (KHN) and Tow-Thomas (TT)

*Corresponding author: Department of Electrical and Electronics Engineering, Dokuz Eylül University, Tinaztepe Campus, Buca, 35160 İzmir-TURKEY

biquads have been implemented using current conveyors, OTRAs, and OTAs [1,16-25]. However, the Fleischer-Tow biquad, which is an improved version of the Tow-Thomas configuration, offers the realization of all 5 different second-order filtering functions, namely low-pass, high-pass, band-pass, notch, and all-pass [26].

In [1], Salama and Soliman introduced an OTRA-based second-order universal filter configuration in addition to the other circuits. It uses 2 active elements and thus it might be more desirable for low power applications. However, the filters derived from the topology in [1] have some disadvantages. One of them is that the circuits employ 3 dynamical elements, namely capacitors, to obtain second-order transfer functions, meaning that the filters are not canonical in the number of capacitors. Since the capacitors occupy a large silicon area on integrated circuits, the resulting filters would be disadvantageous for on-chip applications.

In this study, an OTRA-based Fleischer-Tow biquad, which uses 2 capacitors, is presented for the realization of second-order transfer functions. Therefore, the realized filters are canonical in the number of capacitors and occupy less area on the chip. Additionally, the resonant frequency and quality factor of the filters can be controlled independently. All of the resistors used in the filters were realized by MOS transistors. The resultant MOS-C implementation of the OTRA-based Fleischer-Tow biquad is suitable for full integration.

2. OTRA-based fleischer-tow biquad

The circuit symbol of the OTRA is given in Figure 1. The port relations can be characterized by the following matrix form:

$$\begin{bmatrix} V_p \\ V_n \\ V_z \end{bmatrix} = \begin{bmatrix} 0 & 0 & 0 \\ 0 & 0 & 0 \\ R_m & -R_m & 0 \end{bmatrix} \begin{bmatrix} I_p \\ I_n \\ I_z \end{bmatrix}, \tag{1}$$

where R_m is the transresistance of the OTRA. Since input terminals of this element are internally grounded, most effects of parasitic capacitances at the input disappear. For ideal operation, the transresistance (R_m) approaches infinity, forcing the input currents to be equal. Thus, the OTRA must be used in a feedback configuration in a way that is similar to the classical operational amplifier [1].

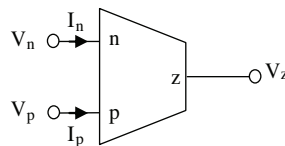


Figure 1. The circuit symbol of the OTRA.

The original operational amplifier-based Fleischer-Tow biquad is given in [22]. The OTRA-based equivalent of this configuration is shown in Figure 2. Routine analysis yields the transfer function as:

$$\frac{V_o}{V_i} = - \frac{\frac{R_8}{R_6} s^2 + \frac{1}{R_1 C_1} \left(\frac{R_8}{R_6} - \frac{R_1 R_8}{R_4 R_7} \right) s + \frac{R_8}{R_3 R_5 R_7 C_1 C_2}}{s^2 + \frac{1}{R_1 C_1} s + \frac{1}{R_2 R_3 C_1 C_2} \cdot \frac{R_8}{R_7}}. \tag{2}$$

The resonant frequency and quality factor are:

$$\omega_0 = \sqrt{\frac{R_8}{R_2 R_3 R_7 C_1 C_2}}, \tag{3}$$

$$Q = \frac{R_1 C_1 \sqrt{R_8}}{\sqrt{R_2 R_3 R_7 C_1 C_2}}. \quad (4)$$

As is seen from Eqs. (3) and (4), the quality factor can be controlled without disturbing the resonant frequency. The sensitivity analysis reveals that the sensitivities of the filter parameters (Q and ω_0) to the passive component values are all less than unity in magnitude. The required condition to realize the 5 basic filtering functions for the Fleischer-Tow biquad is given in the Table.

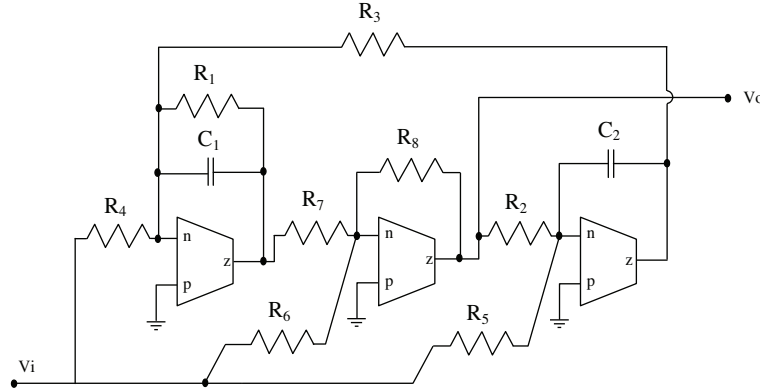


Figure 2. OTRA-based realization of the Fleischer-Tow biquad.

Table. Required condition to realize 5 basic filtering functions for the Fleischer-Tow biquad.

Filter Type	Condition
Low-pass	$R_4 = \infty, R_6 = \infty$
High-pass	$R_4 = R_1, R_5 = \infty, R_6 = R_7 = R_8$
Band-pass	$R_4 = R_1, R_5 = \infty, R_6 = \infty$
Band-reject	$R_4 = \frac{R_6 R_1}{R_8}, R_7 = R_8$
All-pass	$R_4 = \frac{R_1}{2}, R_5 = R_2, R_6 = R_7 = R_8$

3. Nonideality analysis

In practice, the transresistance gain is finite, and, more importantly, it changes with frequency. In this section, the effects of this nonideality inherent in the OTRA on the presented filters are considered. It has been seen that the methods introduced in [1] to compensate for these effects are also applicable to the filters presented in this study. Considering a single pole model for the transresistance gain, R_m , then:

$$R_m(s) = \frac{R_0}{1 + \frac{s}{\omega_0}}. \quad (5)$$

For filter applications that are intended for high frequencies, the transresistance gain, $R_m(s)$, reduces to:

$$R_m(s) \approx \frac{1}{sC_p}, \quad (6)$$

where:

$$C_p = \frac{1}{R_0 \omega_0}. \quad (7)$$

Taking into account this effect, the transfer function in Eq. (2) becomes:

$$\frac{V_o}{V_i} = - \frac{\frac{R_8}{R_6}(sC_1 + sC_p)(sC_2 + sC_p) + \left(\frac{R_8}{R_1R_6} - \frac{R_8}{R_4R_7}\right)(sC_2 + sC_p) + \frac{R_8}{R_3R_5R_7}}{(1 + sC_pR_8)(sC_1 + sC_p)(sC_2 + sC_p) + \frac{1}{R_1}(1 + sC_pR_8)(sC_2 + sC_p) + \frac{R_8}{R_2R_3R_7}}. \quad (8)$$

As is seen, the transfer function has been changed due to nonideal transresistance gain. The effect of this non-ideality can be compensated by connecting a capacitor, C_p , between the output terminal and the noninverting terminal of the second OTRA placed in the middle [1]. The effect of the stray capacitance, C_p , in the other 2 OTRAs with feedback capacitor branches can be absorbed in capacitors C_1 and C_2 , as was done in [1]. In other words, the filters can be designed by taking the magnitude of C_p into consideration, by subtracting its magnitude from the capacitance values of C_1 and C_2 . Thus, the effect of C_p can be absorbed in the integrating capacitances without using any additional elements, and complete self-compensation [1] is achieved for the OTRAs at the left and right sides of the circuit. After these modifications, the circuit shown in Figure 3 was obtained to compensate for the effect of nonideality. It can be shown that this circuit has the same transfer function as in Eq. (2), which is the ideal one, and, therefore, the effect of nonideal R_m is totally compensated with these slight changes in the circuit.

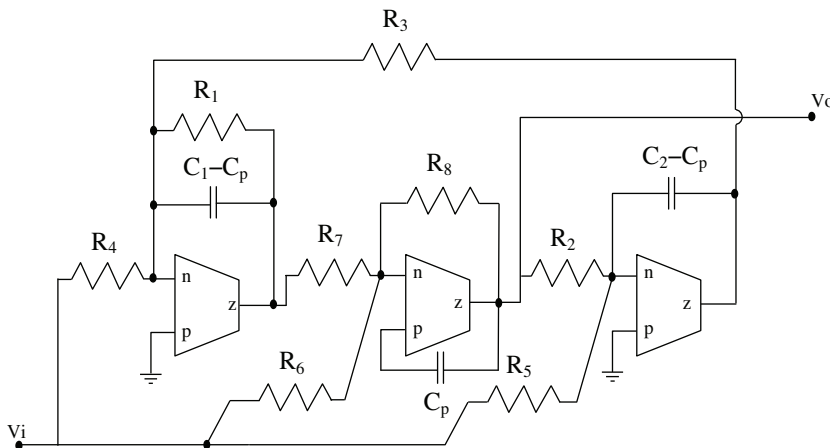


Figure 3. Fleischer-Tow biquad with modifications for compensating the effect of nonideal R_m .

In the following section, the resistors employed in the filter configuration were implemented with MOS transistors. The effect of nonideal R_m and the compensation methods given in this section are still valid for the MOS-C realization of the filter.

4. MOS-C realization of fleischer-tow biquad

It is important to reduce the area of the integrated circuits. In modern CMOS technology, resistors and capacitors occupy large areas on the chips. In this respect, it could be attractive to implement the resistors using transistors, which would reduce the size considerably. It was shown earlier that the internally grounded and current differencing input terminals of OTRA make MOS-C realization possible [1]. That is, the resistors connected to the input terminals of OTRA can easily be implemented using MOS transistors with complete nonlinearity cancellation [1]. The resulting circuit will consist of only MOS transistors and capacitors; hence,

is called MOS-C realization. This will save a significant amount of chip area and lead to circuits that are electronically tunable. That is, the resistance values and hence the related filter parameters can be adjusted by simply changing the bias (gate) voltages [14].

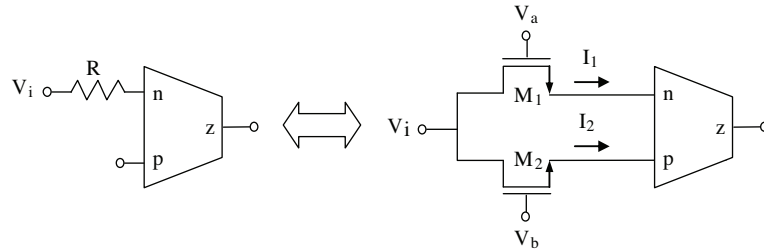


Figure 4. Realizing the resistor connected to the input terminal of OTRA with MOS transistors.

Figure 4 shows how to realize the resistor, which is connected between one of the input terminals of OTRA and a node elsewhere with 2 MOS transistors. Since by definition the input terminals are at the same potential (both virtually grounded), they can both be regarded as one of the terminals of the resistor. Assuming that the 2 NMOS transistors M_1 and M_2 , shown in Figure 4, are matched and operating in the triode region, the currents in that region are given by:

$$I = \mu_n C_{ox} (W/L) (V_G - V_T) (V_D - V_S) + a_1 (V_D^2 - V_S^2) + a_2 (V_D^3 - V_S^3) + \dots \quad (9)$$

Since transistors M_1 and M_2 have equal drain and source voltages, both even and odd nonlinearities are cancelled.

$$I_1 - I_2 = G(V_i - V_2) \quad (10)$$

Due to the current differencing property of the OTRA, the currents in the transistors (I_1 and I_2) are subtracted, yielding nonlinearity cancellation [1]. It should be noted that the 2 NMOS transistors, M_1 and M_2 , should be matched, and they should operate in the ohmic region. The resistance value in Figure 4 can be calculated as [1]:

$$R = \frac{1}{\mu_n C_{ox} (W/L) (V_a - V_b)}, \quad (11)$$

where μ_n is the electron mobility, C_{ox} is the oxide capacitance per unit gate area, W is the effective channel width, L is the effective channel length, and V_a and V_b are the gate voltages.

By replacing each resistor in Figure 2 with the MOS implementation of Figure 4, the fully integrated realization of the Fleischer-Tow biquad, shown in Figure 5, was obtained. The resistor values can be calculated by using Eq. (11). It is easy to show that each resistor in Figure 5 can be electronically controlled with an external voltage. Thus, the quality factor can be adjusted electronically, without disturbing the resonant frequency, with an external control voltage.

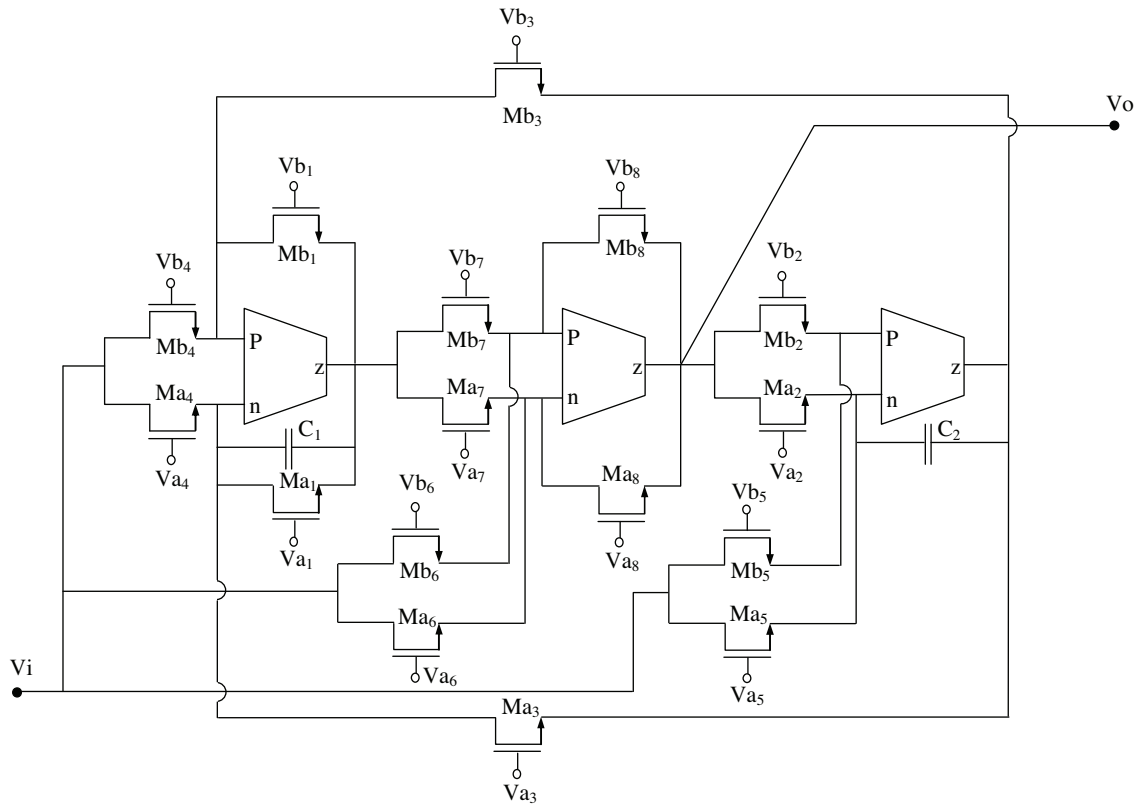


Figure 5. Fully integrated realization of the universal biquads with MOS-C implementation.

5. Simulation results

To verify the theoretical study, the second-order low-pass (LP), high-pass (HP), band-pass (BP), notch or band-stop (BS), and all-pass (AP) filters were simulated with the PSpice program. In the simulations, a CMOS realization of OTRA [1], which is shown in Figure 6, was used with the same transistor aspect ratios as in [1]. Supply voltages were taken as $V_{DD} = 2.5\text{ V}$ and $V_{SS} = -2.5\text{ V}$.

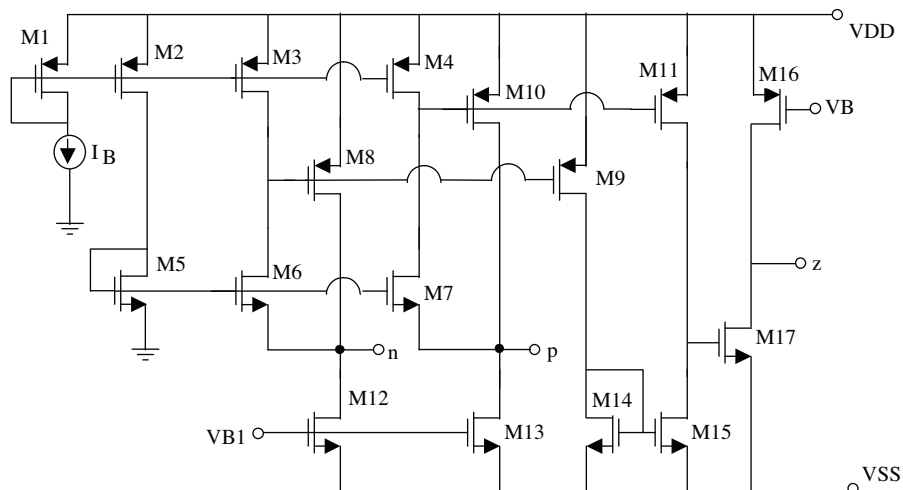


Figure 6. CMOS realization of OTRA.

In the simulation, 0.35- μm TSMC technology parameters were used. According to this parameter set, the gate oxide thickness was given as $T_{ox} = 7.9 \times 10^{-9}$ m. Since the oxide dielectric constant is $\varepsilon_{ox} = 3.46 \times 10^{-11}$ F/m, oxide capacitance was found to be $C_{ox} = \varepsilon_{ox}/T_{ox} = 4.38 \times 10^{-3}$ F. Electron mobility, μ_n , was 436.2 cm^2/Vs for the TSMC 0.35- μm technology.

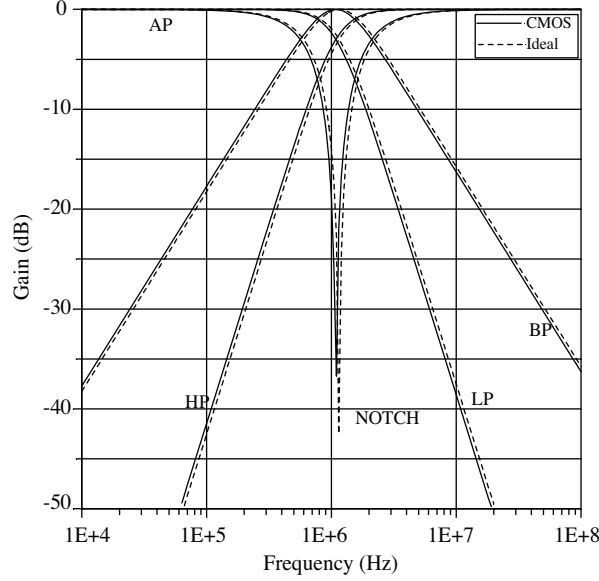


Figure 7. Simulated gain responses of biquadratic filters.

In the simulations, we took $W_{drawn} = 4.2 \mu\text{m}$ and $L_{drawn} = 1.4 \mu\text{m}$ for all transistors realizing the resistors. The effective values for the size of these transistors would be $W = W_{drawn} - 2WINT$ and $L = L_{drawn} - 2LINT$, where $WINT = 7.047 \times 10^{-8}$ m and $LINT = 3.162 \times 10^{-11}$ m. We also took $V_{ai} = 2.3$ V and $V_{bi} = 1.3$ V for all $i = 1, 2, \dots, 8$. Therefore, all of the resistor values were calculated as $R_i \approx 1.9$ k Ω where $i = 1, 2, \dots, 8$ for all filters except the all-pass filter. For the all-pass filter, response R_4 was taken as 0.95 k Ω . For the resistors, which were open circuit condition, the NMOS transistors and the gate voltages were taken as equal. The capacitor values were taken as $C_1 = 50$ pF and $C_2 = 100$ pF. From these values, the theoretical resonant frequency was found as $f_0 \approx 1.184$ MHz. Figure 7 shows the simulation results for all 5 filters. The simulated resonant frequency was equal to $f_0 \approx 1.097$ MHz, which is very close to the theoretical value. The electronically tunable feature of the notch filter was also evaluated and confirmed through PSpice simulations. For this purpose, R_3 was changed by choosing the gate voltage V_{a3} as 1.8 V, 2.0 V, 2.2 V, and 2.4 V while keeping V_{b3} at 1.3 V. These voltages correspond to resistance values of 3.6 k Ω , 2.6 k Ω , 2 k Ω , and 1.65 k Ω for R_3 and in turn the theoretical resonant frequencies of 0.625 MHz, 0.865 MHz, 1.125 MHz, and 1.364 MHz, respectively, with the same values as given above for the passive elements other than R_3 . Figure 8 shows the simulation results for the notch filter, which demonstrate the electronically tunable feature. The simulated resonant frequencies were 0.686 MHz, 0.910 MHz, 1.195 MHz, and 1.410 MHz, respectively, which are very close to theoretical ones.

The electronically tunable feature of the band-pass filter was also evaluated and confirmed through PSpice simulations. For this purpose, R_1 and R_4 were changed by choosing gate voltage V_{a1} as 1.6 V, 1.8 V, 2.0 V, and 2.2 V while keeping V_{b1} at 1.3 V. These voltages correspond to resistance values of 6.0 k Ω , 3.6 k Ω , 2.6 k Ω , and 1.9 k Ω for R_1 . Figure 9 shows the simulation results for the band-pass filter, which demonstrate the

electronically tunable feature. The Q factors were 2.23, 1.34, 0.96, and 0.74, respectively.

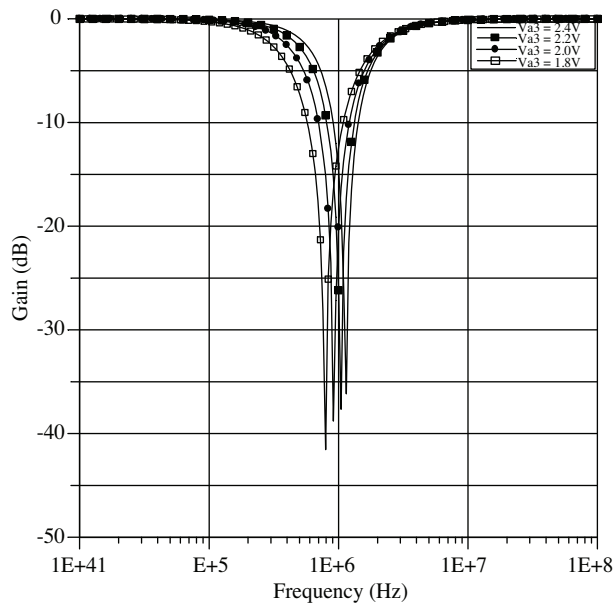


Figure 8. PSpice simulation results showing the electronically tunable feature of the resonant frequency for the notch filter.

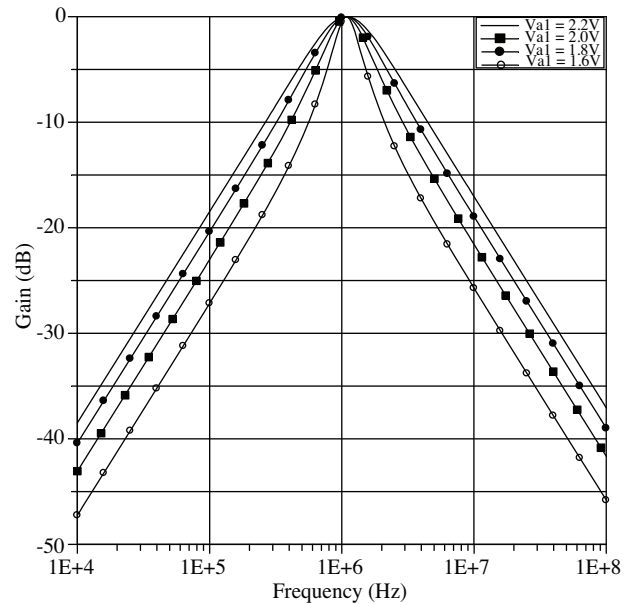


Figure 9. PSpice simulation results showing the electronically tunable feature of the quality factor for the band-pass filter.

6. Conclusion

A circuit configuration to realize 5 different second-order filtering functions, namely low-pass, high-pass, band-pass, notch, and all-pass, was presented. It was derived from a Fleischer-Tow biquad. The presented universal filter employed 3 OTRAs, 2 capacitors, and 8 resistors. Each resistor was implemented with 2 NMOS transistors by making use of the current differencing and internally grounded input terminals of OTRA. This made the presented filters electronically tunable, i.e. filter parameters could be adjusted by changing the bias (gate) voltages. On the other hand, the resulting circuits would consume less area on the chip and therefore be suitable for fully integration. The theoretical analysis was verified with PSpice simulations.

References

- [1] K.N. Salama, A.M. Soliman, "CMOS operational transresistance amplifier for analog signal processing applications", *Microelectronics Journal*, Vol. 30, pp. 235-245, 1999.
- [2] J.J. Chen, H.W. Tsao, C. Chen, "Operational transresistance amplifier using CMOS technology", *Electronics Letters*, Vol. 28, pp. 2087-2088, 1992.
- [3] J.J. Chen, H.W. Tsao, S.I. Liu, W. Chui, "Parasitic-capacitance-insensitive current-mode filters using operational transresistance amplifier", *IEE Proceedings Part G: Circuits, Devices and Systems*, Vol. 142, pp. 186-192, 1995.

- [4] H. Elwan, A.M. Soliman, M. Ismail, "A CMOS Norton amplifier-based digitally controlled VGA for low-power wireless applications", *IEEE Transactions on Circuits and Systems-II: Analog and Digital Signal Processing*, Vol. 48, pp. 245-254, 2001.
- [5] A. Ravindran, A. Savla, I. Younus, M. Ismail, "A 0.8V CMOS filter based on a novel low voltage operational transresistance amplifier", *IEEE International Midwest Symposium on Circuits and Systems*, Vol. 3, pp. 368-371, 2002.
- [6] K.N. Salama, A.M. Soliman, "Universal filters using the operational transresistance amplifiers", *AEU-International Journal of Electronics and Communications*, Vol. 53, pp. 49-52, 1999.
- [7] K.N. Salama, A.M. Soliman, "Novel oscillators using operational transresistance amplifier", *Microelectronics Journal*, Vol. 31, pp. 39-47, 2000.
- [8] U. Cam, "A novel single-resistance-controlled sinusoidal oscillator employing single operational transresistance amplifier", *Analog Integrated Circuits and Signal Processing*, Vol. 32, pp. 183-186, 2002.
- [9] U. Cam, F. Kacar, O. Cicekoglu, H. Kuntman, A. Kuntman, "Novel grounded parallel imittance simulator topologies employing single OTRA", *AEU-International Journal of Electronics and Communications*, Vol. 57, pp. 287-290, 2003.
- [10] S. Kılınç, U. Çam, "A new biquadratic filter configuration employing a single operational transresistance amplifier", *European Conference on Circuit Theory and Design*, Vol. 1, pp. 275-278, 2003.
- [11] U. Cam, C. Cakir, O. Cicekoglu, "Novel transimpedance type first-order all-pass filter using single OTRA", *AEU-International Journal of Electronics and Communications*, Vol. 58, pp. 296-298, 2004.
- [12] F. Kacar, "Operational transresistance amplifier based current-mode all-pass filter topologies", *Applied Electronics*, pp. 149-152, 2009.
- [13] Y.S. Hwang, D.S. Wu, J.J. Chen, C.C. Shih, W.S. Chou, "Realization of high order OTRA MOSFET-C active filters", *Circuits Systems Signal Processing*, Vol. 26, pp. 281-291, 2007.
- [14] Y.S. Hwang, D.S. Wu, J.J. Chen, C.C. Shih, W.S. Chou, "Design of current mode MOSFET-C filters using OTRAs", *International Journal of Circuit Theory and Applications*, Vol. 37, pp. 397-411, 2009.
- [15] R. Pandey, M. Bothra, "Multiphase sinusoidal oscillators using operational trans-resistance amplifier", *IEEE Symposium on Industrial Electronics and Applications*, pp. 371 - 376, 2009.
- [16] W. Kerwin, L. Huelsman, R. Newcomb, "State variable synthesis for insensitive integrated circuit transfer functions", *IEEE J. Solid State Circuits*, Vol. 2, pp. 87-92, 1967.
- [17] L.C. Thomas, "The biquad: Part – Some practical design considerations", *IEEE Trans. Circuit Theory*, Vol. CT-18, pp. 350-257, 1971.
- [18] J. Tow, "Active RC filters – A state-space realization", *Proceedings of the IEEE, Proceeding Letters*, Vol. 56, pp. 1137-1139, 1968.
- [19] R. Senani, V.K. Singh, "KHN-equivalent biquad using current conveyors", *Electronics Letters*, Vol. 31, pp. 626-628, 1995.
- [20] A.M. Soliman, "Kerwin-Huelsman-Newcomb circuit using current conveyors", *Electronics Letters*, Vol. 30, 2019-2020, 1994.

- [21] S. Shah, D.R. Bhaskar, "Design of KHN biquad using operational transconductance amplifier", The 2002 45th Midwest Symposium on Circuit and Systems, Vol. 1, pp. 48-51, 2002.
- [22] A.M. Soliman, "Voltage mode and current mode Tow Thomas biquadratic filters using ICCII", International Journal of Circuit Theory and Applications, Vol. 35, pp. 463-467, 2007.
- [23] A.M. Soliman, "Kerwin-Huelsman-Newcomb circuit using inverting current conveyors", Journal of Active and Passive Electronic Devices, Vol. 3, pp. 273-279, 2008.
- [24] A.M. Soliman, "Generation and classification of Kerwin-Huelsman-Newcomb circuits using the DVCC", International Journal of Circuit Theory and Applications, DOI: 10.1002/cta.503, 2008.
- [25] J. Koton, N. Herencsar, K. Vrba, "KHN-equivalent voltage-mode filters using universal voltage conveyors", International Journal Electron. Commun. (AEU), doi:10.1016/j.aeue.2010.02.005, 2010.
- [26] P.E. Fleischer, J. Tow, "Design formulas for biquad active filters using three operational amplifiers", Proceedings of the IEEE, Proceeding Letters, Vol. 61, pp. 662-663, 1973.